Anatomical and physiological responses Aechmea blanchetiana (Bromeliaceae) induced by silicon and sodium chloride during in vitro culture

Rosiane Cipriano
Federal University of Espirito Santo: Universidade Federal do Espirito Santo
João Paulo Rodrigues Martins (jprmartinss@yahoo.com.br)
Polish Academy of Sciences Institute of Dendrology Kornik: Polska Akademia Nauk Instytut Dendrologii w Korniku https://orcid.org/0000-0003-0554-6793
Lorenzo Toscano Conde
Universidade Federal do Espirito Santo
Mariela Mattos da Silva
Universidade Federal do Espirito Santo
Diolina Moura Silva
Federal University of Espirito Santo: Universidade Federal do Espirito Santo
Andreia Barcelos Passos Lima Gontijo
Universidade Federal do Espirito Santo
Antelmo Ralph Falqueto
Universidade Federal do Espirito Santo

Research Article

Keywords: Bromeliads, Modulated Fluorescence, Tolerance, Plant Tissue Culture, Salinity

Posted Date: April 8th, 2022

DOI: https://doi.org/10.21203/rs.3.rs-1523150/v1

Version of Record: A version of this preprint was published at PeerJ on January 11th, 2023. See the published version at https://doi.org/10.7717/peerj.14624.

Abstract

Salt stress is one of the most severe abiotic stresses affecting plant growth and development. The application of silicon (Si) is an alternative that can increase the tolerance of plants to various types of biotic and abiotic stresses. The objective was to evaluate the effect of salt stress in vitro and the mitigation potential of Si on *Aechmea blanchetiana* plants. For this purpose, plants already established in vitro were transferred to a culture medium with 0 or 14 μM of Si ($CaSiO_3$). After growth for 30 days, a stationary liquid medium containing different concentrations of NaCl (0, 100, 200, or 300 μM) was added to the flasks. Anatomical and physiological analyses were performed after growth for 45 days. The plants cultivated with excess NaCl presented reduced root diameter and effective photochemical quantum yield of photosystem II (PSII) (ΦPSII) and increased non-photochemical dissipation of fluorescence (qN). Plants that grew with the presence of Si also had greater content of photosynthetic pigments and activity of the enzymes of the antioxidant system, as well as higher values of maximum quantum yield of PSII (F_V/F_M), photochemical dissipation coefficient of fluorescence (qP) and fresh weight bioaccumulation of roots and shoots. The anatomical, physiological and biochemical responses, and growth induced by Si mitigated the effect to salt stress of the *A. blanchetiana* plants cultivated in vitro, which can be partly explained by the tolerance of this species to grow in sandbank (*Restinga*) areas.

Introduction

Salinity is responsible for multiple effects that reduce the growth, development, and survival of plants, by means of various mechanisms, including alteration of their hydric relations, deficiency or toxicity of ions, and oxidative stress (Carillo 2018; Hniličková et al. 2019; Morton et al. 2019; Zhu et al. 2019; Chung et al. 2020).

According to Zhao et al. (2019), the hydric stress resulting from increased salinity can impede the roots' access to water in the soil due to the increased osmotic strength of the solution in the soil. During prolonged exposure to high salinity, plants suffer ionic stress, mainly due to sodium chloride, which negatively affects the synthesis of proteins, enzyme activities, and photosynthesis (Munns and Tester 2008; Zhu et al. 2019). Salt stress is accompanied by oxidative stress, leading to the production of reactive oxygen species (ROS). These factors contribute to the deleterious effects of salinity on plants (Acosta- Motos et al. 2015; Zhu et al. 2019). ROS can alter the normal cell metabolism through oxidative damages to the organelles and membranes by lipid peroxidation. Plants' antioxidant systems can be stimulated to combat the oxidative injuries induced by salt stress. These responses include the removal of ROS by enzymes such as ascorbate peroxidase (APX), superoxide dismutase (SOD), and catalase (CAT) (Zhu et al. 2019).

The physiological mechanisms used by plants to minimize the damages caused by stress and reestablish normal growth include processes such as detection and signaling of stress; regulation of metabolism; reduction of stomatal opening, transpiration and photosynthesis; inhibition of cell division and expansion; and changes in plants' morphology, phenology, and allocation of resources (Negrão et al.

2017; Morton et al. 2019). In particular, the regulation of ionic homeostasis involves the sequestration of toxic ions, along with the production and accumulation of organic osmolytes in the cytosol, enabling rapid osmotic adjustment and preventing toxicity (Nikalje et al. 2017; Carillo 2018; Hniličková et al. 2019; Larbi et al. 2020).

Physiological studies of salt stress in vitro are considered a feasible alternative to represent adverse conditions of the external environment (Claeys et al. 2014). Moreover, this method allows controlling the level of stress and reducing the variability of *in vivo* studies (Lawlor 2013). Studies of salt stress in vitro have already been conducted for strawberry (*Cucurbita pepo*) (Harter et al. 2014), *Stevia rebaudiana* Bertoni (Pandey and Chikara 2015; Cantabella et al. 2017; Javed and Gürel 2019), tomato (Zushi and Matsuzoe 2017), and Cape gooseberry (*Physalis peruviana L.*) (Rezende et al. 2018), which have demonstrated the advantages of these techniques for the study of plant physiology.

One alternative to reduce the effects of salt stress on plants is the application of silicon (Si) (Sahebi et al. 2016). Si is considered a beneficial element due to its possibly favorable effects on monocots and eudicots (Martins et al. 2019; Zhu et al. 2019; Cipriano et al. 2021b). Many researchers have reported that Si has attenuating effects on abiotic stresses, such as salinity, drought, and toxicity of heavy metals (Wu et al. 2015; Coskun et al. 2016; Manivannan et al. 2017; Rios et al. 2017; Zhu et al. 2019; Cipriano et al. 2021b).

In vitro cultivation allows studying the physiological functions of Si in plants (Sivanesan and Park 2014; Rezende et al. 2018; Martins et al. 2019; Cipriano et al. 2021a, b). Using Si in the culture medium of plants grown in vitro can increase the growth rate and content of photosynthetic pigments (Asmar et al. 2015; Dias et al. 2017; Rezende et al. 2018; Martins et al. 2019; Cipriano et al. 2021b). The addition of Si can also favor the increased activity of photosynthesis and the antioxidant system (Rodrigues et al. 2017; Manivannan et al. 2018; Ribera-Fonseca et al. 2018; Cipriano et al. 2021b). The favorable effects of Si in the culture medium of plants can be related to increased absorption of nutrients and higher photosynthetic activity, besides enhancing the morphogenetic potential of plants' cells, tissues, and organs (Sivanesan and Park 2014; Zhu et al. 2019; Liu et al. 2019; Liu et al. 2020).

Chlorophyll *a* fluorescence is an important parameter when studying the physiology of plants because it allows measuring the level of stress since the photosynthetic apparatus is extremely sensitive (Kalaji et al. 2016). Among the fluorescence measures, the kinetics of fluorescence of chlorophyll based, or pulse-amplitude modulation (PAM), can detect the performance of that apparatus and evaluate the photosynthetic capacity of plants (Yao et al. 2018). Besides these, studies of the leaf and root anatomy can be important to evaluate the morphological adjustments of plants in response to stressors (Paez-Garcia et al. 2015; Martins et al. 2019).

In the present study, we chose the species *Aechmea blanchetiana* (Baker) L.B. Smith (Bromeliaceae), common name 'orangeade bromeliad', as the plant model because it grows naturally in sandbank (*Restinga*) areas, which are characterized for having high salinity. Si is the most abundant element in the

Earth's crust and is the majority element in the sand (SiO_2) (> 90%) (Costa et al. 2020). In this context, it is crucial to understand which morphophysiological mechanisms allow mitigating the damages induced by salt stress. It is not yet clear how the co-exposure to Si and NaCl can influence the anatomy, performance of the photosynthetic apparatus, and antioxidant enzymes of plants native to sandbank areas. Therefore, the objective of this study was to evaluate the effect of salt stress in vitro induced by NaCl and the mitigation potential of Si in *A. blanchetiana* plants.

Materials And Methods

In vitroculture conditions

Side buds of *A. blanchetiana* with shoot length of approximately 2.5 cm (previously established by in vitromultiplication) were transferred to glass flasks containing MS culture medium (Murashige and Skoog 1962) solidified with 7 g L^{-1} of agar containing 0 or 14 µM of Si ($CaSiO_3$) (Cipriano et al. 2021b). After in vitro growth for 30 days, 30 mL of stationary liquid MS medium, at the original saline solution of 25%, was added to the flasks, supplemented with different concentrations of NaCl (0, 100, 200, or 300 µM), forming a medium with two phases, constituting eight treatments (2 Si x 4 NaCl). The culture medium was added to the aerial part of the plants (shoots). This step was carried out with five explants per flask, and the treatments involving co-exposure to Si and NaCl occurred for 45 days (75 total days). The pH of all the media was adjusted to 5.8 before autoclaving at 120º C, during 20 minutes. The plant material was kept in a growth room with a 16-hour photoperiod under LED lamps (Luminaria LED Slim 36W Bi-Volt 2800 lm) at a temperature of 26 ± 2 ºC.

Analysis of the leaf and root anatomy

After culture for 45 days with Si-NaCl co-exposure, anatomical analyses were performed on six plants per treatment. These were previously collected at random and fixed in an FAA solution (formaldehyde, acetic acid, and 50% ethanol in proportion of 0.5:0.5:9.0) for 72 hours and conserved in 50% ethanol (Johansen 1940). The cross-sections of leaves and roots and paradermal sections were obtained, clarified, and stained as described by Cipriano et al. (2021b). The sections were then observed under an optical microscope (Leica DM5000 B) coupled to a digital camera (Leica EC3) to capture images. For the cross-sections of the leaves and roots, two sections per slide were photographed, with six repetitions per treatment (n = 6). For the paradermal sections, the middle and base regions of the leaf sections were analyzed with six repetitions per treatment (n = 6). The photomicrographs were analyzed using the UTHSCSA-Imagetool® version 3.0 software, calibrated with a microscopic ruler.

The number of metaxylem vessels, the root diameter (µm), and the cell wall thickness of the root exodermis (µm) were determined. The density (0.01 mm^{-2}) and size (µm^2) of the stomata, the thickness of the chlorenchyma (µm) and abaxial and adaxial faces of the epidermis (µm), the area of the sclerenchyma and phloem, along with the diameter of the xylem vessels (µm) were determined in the leaf sections.

Analysis of the mineral nutrient levels

The tissue samples were prepared by drying the entire plants in a forced-air oven for 72 hours at a temperature between 68 and 72 ºC. The analyses were conducted with three repetitions per treatment (*n* = 3). Then the samples were weighed on a precision balance and ground with a Wiley mill, and then placed in glass jars. To determine the concentrations of potassium (K), calcium (Ca), magnesium (Mg), sulfur (S), boron (B), zinc (Zn), manganese (Mn), iron (Fe), and sodium (Na), the samples were digested in a nitric-perchloric acid solution in 4:1 proportion (Sarruge and Haag 1974). The minerals were quantified using inductively coupled plasma-optical emission spectrometry (ICP-OES; PerkinElmer model Optima 8300 DV). The nitrogen (N) content was measured by digestion in sulfuric acid according to the Kjeldahl method (Sarruge and Haag 1974).

Analysis of enzymatic activity

To determine the antioxidant enzyme activities, plants were collected after 45 days of growth. The samples were immediately frozen in liquid nitrogen and stored at -80 C until analysis. The activities of superoxide dismutase (SOD; EC 1.15.1.1), ascorbate peroxidase (APX; EC 1.11.1.11), and catalase (CAT; EC 1.11.1.6) were determined in fully expanded leaves and roots from 5 different samples (*n* = 5). Approximately 0.200 g fresh-frozen leaf or root samples was ground in a mortar and pestle with liquid nitrogen, potassium phosphate buffer (pH 7.8), EDTA 0.1 mM, ascorbic acid 10mM, and PVPP 2% w/v. The homogenate was centrifuged at 13,000 g at 4 °C for 10 min. Aliquots of the supernatant were used for the enzymatic assays described below.

SOD activity was determined by the formation of blue formazan, resulting from the photoreduction of nitrotetrazolium blue chloride (NBT) following Giannopolitis and Ries (1977). SOD activity was detected after incubation under a 15 W fluorescent light for 10 min at 560 nm and expressed as U min^{-1} mg^{-1} protein. CAT activity was determined according to Havir and McHale (1987) by the decay of absorbance at 240 nm, using a 36 mM^{-1} cm^{-1} extinction coefficient and expressed as µmol H_2O_2 min^{-1} mg^{-1} protein. APX activity was determined by the initial ascorbate oxidation by H_2O_2 at 290 nm using a 2.8 mM^{-1} cm^{-1} extinction coefficient and expressed as nmol of ascorbate min^{-1} mg^{-1} protein according to Nakano and Asada (1981). Soluble protein was estimated using Bradford's reagent (Sigma-Aldrich, B6916), by the Coomassie blue dye-binding protein assay, with bovine serum albumin as the standard, according to Bradford (1976), to calculate specific enzyme activity.

Contents of photosynthetic pigments

The contents of photosynthetic pigments were quantified by analyzing 8 randomly chosen fragments (*n* = 8) according to the method described by Martins et al. (2019). The absorbance was measured using a Genesys™ 10S UV-Vis spectrophotometer (Thermo Fisher Scientific, West Palm Beach, FL, USA), conducted at λ = 470, 645 and 663 nm for carotenoids (Car), chlorophyll *b* (Chl *b*), and chlorophyll *a* (Chl

a), respectively. The content of pigments was calculated according to Arnon (1949) and Wellburn (1994) and expressed as μg g^{-1} FW (fresh weight).

Measurement of modulated chlorophyll *a* fluorescence

The analyses of photosynthetic efficiency were carried out between 8:00 and 10:00 a.m. by measuring the modulated chlorophyll *a* fluorescence with a PAM-2500 Walz portable chlorophyll fluorometer, following the method described by Ögren and Baker (1985) and Schreiber (1986). The measurements were carried out on 12 plants per treatment (n = 12), according to the method of Ögren and Baker (1985) and described further in Cipriano et al. (2021b). The following variables were obtained: F_V/F_M, ETR, ΦPSII, qN, qP, qL, NPQ, ΦNPQ, and ΦNO.

Analysis of the growth traits

After 45 days of co-exposure to Si-NaCl, the fresh weight was evaluated of the shoots and roots (g $plant^{-1}$) with 5 repetitions per treatment (n = 5), with each repetition consisting of 5 plants.

Statistical analysis

The experimental design was completely randomized in a 4x2 factorial scheme: 4 NaCl concentrations (0, 100, 200, or 300 μM) and 2 Si concentrations (0 or 14 μM). The data obtained were submitted to analysis of variance (ANOVA), and the means were compared by the Tukey test at 5% probability, using the SISVAR 5.4 software (Ferreira 2011).

Results

Anatomical analysis

Significant differences were observed in the anatomical traits of the roots. The root diameter was influenced only by the saline concentration, being largest at 100 μM and smallest at 0 μM and 300 μM NaCl (Figs. 1A-I). The thickness of the cell walls of the exodermis was influenced by both factors evaluated. In the absence of Si, the exodermal cell wall thickness was smaller with all NaCl concentrations compared to the control. In turn, in the presence of Si, the values were similar regardless of the concentration of NaCl applied. However, the cell walls were thinner in relation to those of the roots in the control treatment (Figs. 1A-H and 1I). The number of metaxylem vessels did not differ among the treatments (5.94 ± 0.55).

In the paradermal leaf sections, the stomatal density of the basal region was influenced only by the NaCl concentration. In this region, there was a decrease in the number of stomata with increasing NaCl concentration (Fig. 2A-H and 2R). However, the density and size of the stomata of the middle region of the leaves were influenced only by exposure to Si. When cultivated with 14 μM Si, the plants presented a reduction of 14% in the stomatal density and 3% in the stomatal size(Fig. 2I-P and 2S-T).

In the leaf cross-sections, the thickness of the adaxial and abaxial faces of the leaf epidermis (μm) was influenced only by the NaCl concentration, being largest at the concentration of 300 μM NaCl (Figs. 3 and 4A-B). Plants cultivated in NaCl presence had thicker chlorenchyma, mainly at the concentration of 200 μM NaCl (Figs. 3 and 4C). The area of the sclerenchyma (1007.5 μm^2 ± 59.86), area of the phloem (587.08 μm^2 ± 26.01), and diameter of the xylem vessels (9.90 ± 0.36) did not differ significantly among the treatments (Fig. 3).

Contents of nutrients

The contents of Mg, S, Na, and B were influenced by both variation factors, with a significant interaction between them. Plants grown in a medium with Si and NaCl, irrespective of the concentration, had lower content of S. On the other hand, higher NaCl concentration promoted increased Mg, Na, and B contents (Figs. 5A-D). The contents of Fe, Zn, Mn, and Ca, and the Na/K ratio, were influenced by both variation factors, but Si and NaCl acted independently. Lower contents of Fe, Zn, Mn, and Ca were observed in NaCl presence. A higher Na/K ratio was associated with greater salt concentration. The content of K did not differ significantly between the different concentrations of NaCl (2.027 ± 0.098), nor did the content of N (1.75 ± 0.073). The presence of Si increased the contents of Zn, Mn, Ca, and N and the Na/ K ratio. Finally, the content of Fe (179.97 ± 8.77) did not differ in function of the Si concentration (Figs. 6A-B).

Antioxidant enzyme activity

The activity of SOD and CAT, both shoots and roots, was influenced by both variation factors. The activity of SOD was higher in the plants cultured with Si and increased in the function of rising NaCl concentration. The greatest activity of SOD occurred in the presence of 300 μM NaCl, both in the leaves and roots (Figs 7A-B). The activity of CAT was greatest in the plants grown with Si and increased with rising concentrations of NaCl (200 and 300 μM NaCl) (Figs. 7C-D). Both the factors influenced the activity of APX, but they acted separately. The activity of APX was highest with greater concentrations of NaCl in the plants cultivated in medium supplemented with Si, both in the leaves and roots (Figs. 7E-F).

Contents of photosynthetic pigments

Only the treatment with Si influenced the contents of photosynthetic pigments. Plants cultivated with Si had higher contents of Chl *a*, Car, and Chl total, but there was no alteration in Chl *b* and Chl *a/b* in the leaves of *A. blanchetiana* plants cultured in vitro (Fig. 8).

Analysis of modulated chlorophyll fluorescence

The variables ΦPSII and ETR were influenced only by NaCl, with lower values associated with rising NaCl concentration (Figs. 9A-B). In turn, NPQ and F_V/F_M were influenced by Si, presenting lower NPQ and higher F_V/F_M in the plants grown in medium supplemented with Si (Figs. 9C-D). qP, qL, qN, ΦNPQ, ΦNO were all influenced by both variation factors. Among the plants cultivated without Si, no significant differences were observed for qPand qL. However, at the highest concentration of NaCl, there were

increases of qN and ΦNPQ. The highest values of ΦNO were obtained in the control plants and those grown with 100 µM NaCl and the lowest at 200 µM NaCl. Among the plants cultivated in the presence of Si, the lowest values of qP and qL were observed in those grown with 200 µM NaCl, as was the case for qN. However, the greatest values of qN were obtained in the plants cultivated in a medium containing 300 µM NaCl. The absence of NaCl was associated with the highest values of qPandqL. No changes in ΦNO and ΦNPQ were observed between treatments (Fig. 10).

Analysis of growth

The fresh weights of the roots and shoots were influenced by both variation factors. Among the plants grown without Si, the shoot and root weights declined with increasing NaCl concentration. However, among the plants cultivated in a medium with Si, the shoot's fresh weight increased in the presence of 200 µM NaCl, while the root's fresh weight increased in the plants receiving 100 µM NaCl. Overall, the fresh weights of the shoots and roots were greater in the plants cultivated in Si and higher concentrations of NaCl in comparison with the plants grown without Si (Fig. 11).

Discussion

The *A. blanchetiana* plants cultivated under the in vitro conditions imposed showed different anatomical and physiological responses due to the presence or absence of Si and the variation in concentrations of NaCl. The morphophysiological responses induced by Si had an attenuating effect on salt stress, through anatomical alterations, increased content of photosynthetic pigments, and greater activity of the enzymes of the antioxidant system, besides their contribution to enhance the performance of the photosynthetic apparatus.

The root and leaf anatomy of the plants was in accordance with the previous description of Martins et al. (2018). The reduction of the diameter of the root cross-sections under salt stress conditions found in this study might have resulted from reductions in the size and number of cells, especially in the internal cortex. The alterations of the cell size can be related to resistance to salt stress since smaller cells can indicate an essential response to increase the water potential, possibly contributing to more effective maintenance of turgor under water deficit (Munns and Tester 2008; Terletskaya et al. 2019). Reduced root diameters can be a sign of adaptation to the high pressure of the water column on the conductor system (Rewald et al. 2013; Terletskaya et al. 2019).

The thickening of the cell wall of the exodermis of the roots was modulated by the concentrations of NaCl. This thickening occurs naturally by deposition of lignin and/or suberin, and the degree of thickening can moderate the uptake and translocation of mineral nutrients to the entire plant (Martins et al. 2019). The exposure to excessive NaCl in the shoots induced a thinner exodermis in the roots, which could have been the key to the tolerance of excess NaCl in the shoots. The thinner exodermis permitted a greater flow of nutrients from the culture medium to the shoots, which in turn improved the nutritional balance. Furthermore, in the presence of Si, the thickness of the exodermis was smaller compared to the

control plants, showing that Si can act as a modulator and contribute positively to the absorption of nutrients, as previously described by Martins et al. (2019) in *A. blanchetiana* plants grown in vitro with Si.

In the leaves, the direct exposure to NaCl at the leaf base reduced the stomatal density. Besides this, the epidermis was thicker in the plants exposed to salt. These responses together suggest a morphological adjustment to control the entry of NaCl through the symplastic and transcellular veins (Morton et al. 2019). Considering that plants can also absorb nutrients through the leaves, an increase in the thickness of the epidermis can function as a mechanism to control the absorption of excessive NaCl (Mahmood et al. 2019). It has been suggested that the movement of nutrients to the interior of plants can involve diffusion through the cuticle and absorbed by leaf cells. Absorption through the stomatal pore can also occur since the stomata act as potential pathways for the movement of nutrients applied to the leaves (Li et al. 2019).

In the middle region of the leaves, the stomatal density was greater than in the base region, as previously observed by Santos et al. (2020). However, a comparison of the treatments revealed that Si could influence the morphology of the stomata of other leaf regions. The morphophysiological modulations in the middle leaf region in plants grown with Si, such as smaller stomatal density and size, might have occurred to reduce the osmotic stress (Mahmoudi et al. 2019; Morton et al. 2019). This reduction resulting from the action of Si might be a mechanism to maintain the prompt functioning of the stomata for osmotic control. The size of the stomata is related to their functionality because smaller guard cells respond (open/close) faster than larger ones, and consequently maintain the stomatal conductance (Rouphael et al. 2017). Another alteration observed in this study was an increase in the thickness of the chlorenchyma, apparently related to a trade-off mechanism in which the smaller leaf area is offset by the greater thickness of this tissue (Pereira et al. 2016). This capacity for the protection of the photosynthetic tissues permits maintenance of the plant's biomass production (Pereira et al. 2016; Ribeiro et al. 2019).

The excess of NaCl altered the content of mineral nutrients in *A. blanchetiana*, namely reduction of the contents of the macronutrients S and Ca and the micronutrients Fe, Zn, and Mn. The excessive accumulation of Na^+ competitively inhibits the absorption of other cations, including K^+, Ca^{2+}, and Fe^{2+}, leading to an imbalance in cell homeostasis, oxidative stress, and interference in the functions of Ca^{2+} and K^+ (Kim et al. 2021). Besides this, the limited availability of Ca can reduce the tolerance of plants to salt stress since this is involved in the gene induction of tolerance to salt stress and regulation of the antioxidant defense (Liu et al. 2019). K plays a fundamental role in synthesizing proteins, photosynthesis, and the activity of glycolytic enzymes in plants (Liu et al. 2019). Therefore, we suggest that reducing the contents of S, Ca, Fe, Zn, and Mn reduced the stress tolerance of the plants, generating oxidative stress and affecting the functioning of the photosynthetic apparatus.

The modulations of the contents of mineral nutrients in *A. blanchetiana* promoted by Si contributed to improve the nutritional balance and mitigated the damages caused by the toxicity of NaCl in the leaf cells. The increase promoted by Si in the contents of the nutrients Ca, B, Zn, Mn, N, and Mg was probably due to the thinner exodermis in the roots, modulated by Si, which allowed greater absorption of these

nutrients. The resulting better nutritional balance contributed to increase the content of photosynthetic pigments and the activity of the enzymes of the antioxidant system (SOD, APX, and CAT). This promoted the protection of the plants' tissues against oxidative damages to the membrane under salt stress, thus alleviating the toxicity of salt and increasing the growth of the *A. blanchetiana* plants. These nutrients are structural components of the chlorophyll molecule and play a role in forming the amino acids necessary for the processes of the antioxidant defense system, acting as enzymatic cofactors, for example (Rahman et al. 2016; Tewari et al. 2019; Santos et al. 2021). Besides this, the greater activity of the antioxidant system enzymes leads to lower degradation of chlorophyll (Gong et al. 2018). Higher B content contributes to increasing the defense of the antioxidant system and diminishing oxidative stress (Rahman et al. 2021). The increase in the activity of antioxidant enzymes is also responsible for reducing oxidative stress and eliminating the ROS produced during salt stress (Tewari et al. 2019; Zhang et al. 2019; Chung et al. 2020; Kim et al. 2021). In this study, the activity of the antioxidant enzymes was greater in the shoots than in the roots of the plants cultivated in the medium supplemented with Si. This result indicates that the direct exposure to NaCl on the leaves had an impact, generating oxidative stress.

Even though the presence of Na caused stress, as indicated by the biochemical alterations described, this element also appears to play a fundamental role in the metabolism of *A. blanchetiana* plants, and its absorption in minimum quantities seems to have occurred. Plants grown in the 0 µM NaCl + 14 µM Si condition had greater content of Na than in the control plants (Na added only in the form of Na-EDTA in the MS medium). Other studies have shown that *A. blanchetiana* has crassulacean acid metabolism (CAM) for the fixation of carbon under adverse conditions (Chaves et al. 2014; Krause et al. 2016). We suggest that even in in vitro conditions, *A. blanchetiana* plants can have some CAM behavior level, such as reducing leaf area making the leaves more compact. Plants that use CAM metabolism can require sodium ions (Na^+) (Scholl et al. 2020). In this species, Na^+ seems to be fundamental for the regeneration of phosphoenolpyruvate, the substrate for initial carboxylation in plants with C_4 and CAM metabolism (Scholl et al. 2020). CAM metabolism is a mechanism that protects against increased salinity, but the most critical tolerance mechanism can be the accumulation of ions in leaf vacuoles for osmotic adjustment (Montero et al. 2018). In halophytes, the accumulation of Na and its compartmentalization in vacuoles modulate the osmotic potential and help guarantee water absorption under salt stress conditions (Zeng et al. 2015). The Na ions stimulate growth by promoting cell expansion and partially substitute K ions as an osmotically active solute (Hussain et al. 2010). This modulation of the content of Na^+ can partly explain the salt tolerance and thus the existence of *A. blanchetiana* in the sandbank (*Restinga*) region studied here. Furthermore, this can also explain the increase in the Na/ K ratio with higher salt concentration and the presence of Si observed in this study, which has been confirmed to be one of the main determinants of resistance to salts (Liu et al. 2020). Despite this increase in the Na/ K ratio, the use of Si was responsible for modulating the competitive absorption between Na and K and maintaining the balance in the intercellular distribution of K in the *A. blanchetiana* plants since the content of K was not different between the treatments.

The morphophysiological modulations promoted by Si, such as the greater activity of the enzymes SOD, APX, and CAT, reduced the stress on the photosynthetic apparatus, as demonstrated by the analysis of the chlorophyll *a* fluorescence. The plants grown in the medium supplemented with Si had the highest values of qP and qL, implying a more remarkable ability for photochemical conversion and transfer of electrons from PSII (Wang et al. 2018). This suggests that even though the plants grown with high NaCl suffered photodamage, the Si was able to ameliorate this damage by maintaining a proper balance of nutrients, as well as enhancing the activity of the antioxidant system, impeding oxidative damages to the photosystems (Liu et al. 2020). The Si also contributed to maintain the electron transport, as evidenced by the higher F_V/F_M ratio, indicating greater potential photochemical activity of PSII (Lotfi et al. 2018). Factors for the photosynthetic apparatus's functioning were also evidenced by the lower values of the parameters of non-photochemical quenching, such as qN, ΦNPQ, and NPQ, in comparison with the plants grown without Si. These responses helped to reduce the damages to the plants caused by the stress, which in turn helped to maintain the plants' growth since they had greater fresh weight when cultivated with higher concentrations of NaCl. The excess of NaCl in plants grown without Si caused increases of qN, ΦNPQ, and ΦNO, leading to over-reduction of the photosynthetic electron transport chain, excess excitation energy, and consequently reduction of the photochemical step and biochemical processes. The increase of ΦNPQ indicates that the regulation of the excitation energy loss occurred by dissipation of the heat involving the mechanisms dependent on ΔpH and zeaxanthin and by means of the xanthophyll cycle (Wang et al. 2018; Shu et al. 2019). Furthermore, the increase of ΦNO indicates that this energy loss did not involve the action of trans-thylakoid ΔpH and zeaxanthin, meaning the excess flow of energy was out of control (Yao et al. 2018; Wang et al. 2018).

The increase of the stress level caused by NaCl affected the functioning of the photosynthetic apparatus by reducing the values of ΦPSII and ETR. The decrease might have partly inhibited the transport of electrons and effective photochemical activity of PSII and increased the formation of ROS since the activity of the antioxidant system was affected. This reduction indicates a smaller density of the flow of photons absorbed by PSII (Wang et al. 2018). These responses induced by excess of NaCl in the absence of Si caused a reduction of the plants' growth. The decline of the fresh and dry weights of the leaves and roots, and thus the reduction in the plants' growth, are symptoms commonly observed in plants under salt stress (Dias et al. 2017). This result can be attributed to the osmotic effect of the salt solution beyond the roots, as well as an imbalance in the absorption and assimilation of nutrients (Dias et al. 2017; Rezende et al. 2018).

Conclusion

In in vitro conditions, NaCl acted to stunt the growth of the *A. blanchetiana* plants since it affected the plants' anatomy, absorption of nutrients, and physiology. These plants presented tolerance responses by implementing various mechanisms to deal with salt stress, such as thinner walls of the exodermis, reduced stomatal density, and increased non-photochemical dissipation of fluorescence. The application of Si reduced the damages generated by stress through modulation of the root anatomy, enabling greater

uptake of nutrients essential for the antioxidant system's activity. The greater enzymatic activity reduced the oxidative stress and enabled alterations of the functioning of the photosynthetic apparatus. These modulations contributed to minimizing the damages to the plants caused by the stress, as proved by the chlorophyll *a* fluorescence.

Abbreviations

ΦPSII = Y(II) = Φ(II) – Effective photochemical quantum yield of PSII; ETR – Rate of linear electron flow; F_V/F_M – maximum quantum yield of PSII; NPQ – non-photochemical fluorescence dissipation; PSII – photosystem II; qP – photochemical quenching; qL – photochemical fluorescence quenching assuming interconnected PSII antennae; qN – non-photochemical quenching; ΦNPQ – quantum yield induced light (ΔpH and zeaxanthin-dependent) from non-photochemical fluorescence dissipation; ΦNO – quantum yield of non-regulated energy dissipation.

Declarations

Acknowledgments: The authors acknowledge the scholarship granted by CAPES (Coordination for the Improvement of Higher Education Personnel). The authors also acknowledge Luiz Carlos de Almeida Rodrigues for technical assistance in making the figures.

Author contributions: RC, JPRM, and LTC performed experiments. MMS and DMS performed the analysis of enzymatic activity. RC and JPRM wrote the manuscript and performed the statistical analysis. ARF and ABPLG provided the structure and contributed to the design and interpretation of the results. All the authors have read and approved the manuscript.

Ethics declarations

Conflict of interest: The authors have not disclosed any potential competing conflict of interest.

References

1. Acosta-Motos JR, Díaz-Vivancos P, Álvarez S, Fernández-García N, Sánchez- Blanco MJ, Hernández JA (2015) NaCl-induced physiological and biochemical adaptative mechanisms in the ornamental *Myrtus communis* L. plants. J Plant Physiol 183:41–51. https://doi.org/10.1016/j.jplph.2015.05.005
2. Arnon DI (1949) Copper enzymes in isolated chloroplasts. Polyphenoloxidase in *Beta vulgaris*. Plant Physiol 24:1–15. https://doi.org/10.1104/pp.24.1.1
3. Asmar AS, Soares JDR, Silva RAL, Pasqual M, Pio LAS, Castro EM (2015) Anatomical and structural changes in response to application of silicon (Si) *in vitro* during the acclimatization of banana cv. 'Grand Naine'. Aust J Crop Sci 9:1236–1241
4. Bradford MM (1976) A rapid and sensitive method for the quantitation of microgram quantities of protein utilizing the principle of protein–dye binding. Anal Biochem 72:248–254.

https://doi.org/10.1016/0003-2697(76)90527-3

5. Brundrett MC, Enstone DE, Peterson CA (1988) A berberine-aniline blue fluorescent staining procedure for suberin, lignin, and callose in plant tissue. Protoplasma 146:133–142. https://doi.org/10.1007/BF01405922
6. Cantabella D, Piqueras A, Acosta-Motos JR, Bernal-Vicente A, Hernández JA, Díaz-Vivancos P (2017) Salt-tolerance mechanisms induced in *Stevia rebaudiana* Bertoni: Effects on mineral nutrition, antioxidative metabolism and steviol glycoside content. Plant Physiol Biochem 115:484–496. https://doi.org/ 10.1016/j.plaphy.2017.04.023
7. Carillo P (2018) GABA Shunt in Durum Wheat. Front Plant Sci 9:100. https://doi.org/10.3389/fpls.2018.00100
8. Chaves CJN, Leal BSS, Lemos-Filho JP (2015) Temperature modulation of thermal tolerance of a CAM-tank bromeliad and the relationship with acid accumulation in different leaf regions. Physiol Plant 154:500–510. https://doi.org/10.1111/ppl.12295
9. Chung YS, Kim K-S, Hamayun M, Kim Y (2020) Silicon Confers Soybean Resistance to Salinity Stress Through Regulation of Reactive Oxygen and Reactive Nitrogen Species. Front Plant Sci 10:1725. https://doi.org/10.3389/fpls.2019.01725
10. Cipriano R, Martins JPR, Rodrigues LCA, Falqueto AR, Gontijo ABPL (2021a) Impact of saline solution on growth and photosystem II during *in vitro* cultivation of *Bromelia antiacantha* (Bromeliaceae). Rodriguésia 72. https://doi.org/10.1590/2175-7860202172018
11. Cipriano R, Martins JPR, Conde LT, Moreira SW, Clairvil E, Braga PCS, Gontijo ABPL, Falqueto AR (2021b) Anatomical, physiological, and biochemical modulations of silicon in *Aechmea blanchetiana* (Bromeliaceae) cultivated *in vitro* in response to cadmium. Plant Cell Tissue Organ Cult 147:271–285. https://doi.org/10.1007/s11240-021-02122-2
12. Claeys H, Landeghen SV, Dubois M, Maleux K, Inzé D (2014) What is stress? Dose-response effects in commonly used *in vitro* stress assays. Plant Physiol 165:519–527. https://doi.org/10.1104/pp.113.234641
13. Coskun D, Britto DT, Huynh WQ, Kronzucker HJ (2016) The role of silicon in higher plants under salinity and drought stress. Front Plant Sci 7:1072. https://doi.org/10.3389/fpls.2016.01072
14. Costa WS, Yamamura RHR, Morcelli CPR, Sígolo JB (2020) Adição de resíduo de marmoraria em pastas cimentícias, avaliação de suas propriedades mecânicas e caracterização química. INOVAE - Journal of Engineering Architecture and Technology Innovation 8:1–18)
15. Dias GMG, Soares JDR, Ribeiro SF, Martins AD, Paqual M, Alves E (2017) Morphological and physiological characteristics *in vitro* anthurium plantlets exposed to silicon. Crop Breed Appl Biotechnol 17:18–24. https://doi.org/10.1590/1984-70332017v17n1a3
16. Ferreira DF (2011) Sisvar: a computer statistical analysis system. Cienc Agrotec 35:1039–1042. https://doi.org/ https://doi.org/10.1590/S1413-70542011000600001
17. Giannopolitis CN, Ries SK (1977) Superoxide dismutases: I. Occurrence in higher plants. Plant Physiol 59:309–314. https://doi.org/10.1104/pp.59.2.309

18. Gong DH, Wang GZ, Si WT, Zhou Y, Liu Z, Jia J (2018) Effects of salt stress on photosynthetic pigments and activity of ribulose-1,5-bisphosphate carboxylase/oxygenase in *Kalidium foliatum*. Russ J Plant Physiol 65:98–103. https://doi.org/10.1134/S1021443718010144
19. Harter LSH, Harter FS, Deuner C, Meneghello GE, Villela FA (2014) Effect of salinity on physiological performance of mogango seeds and seedlings. Hortic Bras 32:80–85. https://doi.org/ 10.1590/S0102- 5362014000100013
20. Havir EA, McHale NN (1987) Biochemical and developmental characterization of multiple forms of catalase in tobacco leaves. Plant Physiol 84:450–455. https://doi.org/10.1104/pp.84.2.450
21. Hniličková H, Hnilička F, Orsák M, Hejnák V (2019) Effect of salt stress on growth, electrolyte leakage, Na^+ and K^+ content in selected plant species. Plant Soil Environ 65:90–96. https://doi.org/10.17221/620/2018-PSE
22. Hussain K, Nisar MF, Majeed A, Nawaz K, Bhatti KH, Afghan S, Shahazad A, Zia-ul-Hussnian S (2010) What molecular mechanism is adapted by plants during salt stress tolerance? Afr J Biotechnol 9:416–422
23. Javed R, Gurel E (2019) Salt stress by NaCl alters the physiology and biochemistry of tissue culture-grown *Stevia rebaudiana* Bertoni. Turk J Agric For 43:11–20. . doi:10.3906/tar-1711-71
24. Johansen DA (1940) Plant microtechnique. Nature 147:222. https://doi.org/10.1038/147222b0
25. Kalaji HM, Jajoo A, Oukarroum A, Brestic M, Zivcak M, Samborska IA, Cetner MD, Łukasik I, Goltsev V, Ladle RJ (2016) Chlorophyll *a* fluorescence as a tool to monitor physiological status of plants under abiotic stress conditions. Acta Physiol Plant 38:102. https://doi.org/ 10.1007/s11738-016-2113-y
26. Kim B, Lee H, Song YH, Kim H (2021) Effect of salt stress on the growth, mineral contents, and metabolite profiles of spinach. J Sci Food Agric 101:3787–3794. https://doi.org/10.1002/jsfa.11011
27. Krause GH, Winter K, Krause B, Virgo A (2016) Protection by light against heat stress in leaves of tropical crassulacean acid metabolism plants containing high acid levels. Funct Plant Biol 43:1061–1069. https://doi.org/10.1071/fp16093
28. Lawlor DW (2013) Genetic engineering to improve plant performance under drought: physiological evaluation of achievements, limitations, and possibilities. J Exp Bot 64:83–108. https://doi.org/ 10.1093/jxb/ers326
29. Larbi A, Kchaoub H, Gaaliche B, Gargouri K, Boulal H, Morales F (2020) Supplementary potassium and calcium improves salt tolerance in olive plants. Sci Hortic 260:108912. https://doi.org/10.1016/J.SCIENTA.2019.108912
30. Li C, Wang P, Van der Ent A, Cheng M, Jiang H, Lund Read T, Lombi E, Tang C, Jonge MD, Menzies NW, Kopittke PM (2019) Absorption of foliar-applied Zn in sunflower (*Helianthus annuus*): importance of the cuticle, stomata and trichomes. Ann Bot 123:57–68. https://doi.org/10.1093/aob/mcy135
31. Liu B, Soundararajan P, Manivannan A (2019) Mechanisms of Silicon-Mediated Amelioration of Salt Stress in Plants. Plants 8:307. https://doi.org/10.3390/plants8090307

32. Liu C, Zhao X, Yan J, Yuan Z, Gu M (2020) Effects of Salt Stress on Growth, Photosynthesis, and Mineral Nutrients of 18 Pomegranate (*Punica granatum*) Cultivars. Agronomy 10:27. https://doi.org/10.3390/agronomy10010027
33. Lotfi R, Kalaji HM, Valizadeh GR, Khalilvand Behrozyar E, Hemati A, Gharavi-Kochebagh P, Ghassemi A (2018) Effects of humic acid on photosynthetic efficiency of rapeseed plants growing under different watering conditions. Photosynthetica 56:962–970. https://doi.org/10.1007/s11099-017-0745-9
34. Mahmood YA, Ahmed FW, Juma SS, Al-Arazah AA (2019) Effect of solid and liquid organic fertilizer and spray with humic acid and nutrient uptake of nitrogen, phosphorus and potassium on growth, yield of cauliflower. Plant Arch 19:1504–1509
35. Mahmoudi H, Salah IB, Zaouali W, Hamrouni L, Gruber M, Ouerghi Z, Hosni K (2020) Priming-induced changes in germination, morpho-physiological and leaf biochemical responses of fenugreek (*Trigonella foenum-graecum*) under salt stress. Plant Biosyst 154:601–614. https://doi.org/10.1080/11263504.2019.1651785
36. Manivannan A, Ahn YK (2017) Silicon regulates potential genes involved in major physiological processes in plants to combat stress. Front Plant Sci 8:1346. https://doi.org/10.3389/fpls.2017.01346
37. Manivannan A, Soundararajan P, Cho YS, Park JE, Jeong BR (2018) Sources of silicon influence photosystem and redox homeostasis- related proteins during the axillary shoot multiplication of *Dianthus caryophyllus*. Plant Biosyst 152:704–710. https://doi.org/10.1080/11263504.2017.1320312
38. Martins JPR, Rodrigues LCA, Santos ER, Batista BG, Gontijo A, Falqueto AR (2018) Anatomy and photosystem II activity of *in vitro* grown *Aechmea blanchetiana* as affected by 1-naphthaleneacetic acid. Biol Plant 62:211–221. https://doi.org/10.1007/s10535-018-0781-8
39. Martins JPR, Rodrigues LCA, Silva TS, Santos ER, Falqueto AR, Gontijo ABPL (2019) Sources and concentrations of silicon modulate the physiological and anatomical responses of *Aechmea blanchetiana* (Bromeliaceae) during *in vitro* culture. Plant Cell Tissue Organ Cult 137:397–410. https://doi.org/10.1007/s11240-019-01579-6
40. Martins JPR, Vasconcelos LL, Braga PCS, Rossini FP, Conde LT, Rodrigues LCA, Falqueto AR, Gontijo ABPL (2020) Morphophysiological responses, bioaccumulation and tolerance of *Alternanthera tenella* Colla (Amaranthaceae) to excess copper under *in vitro* conditions. Plant Cell Tissue Organ Cult 143:303–318. https://doi.org/10.1007/s11240-020-01917-z
41. Morton MJL, Awlia M, Al-Tamimi N, Saade S, Pailles Y, Negrão S, Tester M (2019) Salt stress under the scalpel–dissecting the genetics of salt tolerance. Plant J 97:148–163. https://doi.org/10.1111/tpj.14189
42. Montero E, Francisco AM, Montes E, Herrera A (2018) Salinity induction of recycling Crassulacean acid metabolism and salt tolerance in plants of *Talinum triangulare*. Ann Bot 121:1333–1342. https://doi.org/10.1093/aob/mcy030

43. Munns R, Tester M (2008) Mechanisms of salinity tolerance. Annu Rev Plant Biol 59:651–681. https://doi.org/10.1146/annurev.arplant.59.032607.092911
44. Murashige T, Skoog F (1962) A revised medium for rapid growth and bioassays with tobacco tissue cultures. Physiol Plant 15:473–497. https://doi.org/10.1111/j.1399-3054.1962.tb08052.x
45. Nakano Y, Asada K (1981) Hydrogen peroxide is scavenged by ascorbate specific peroxidase in spinach chloroplasts. Plant Cell Physiol 22:867–880. https://doi.org/10.1093/oxfordjournals.pcp.a076232
46. Negrão S, Schmöckel SM, Tester M (2017) Evaluating physiological responses of plants to salinity stress. Ann Bot 119:1–11. https://doi.org/10.1093/aob/mcw191
47. Nikalje GC, Srivastava AK, Pandey GK, Suprasanna P (2017) Halophytes in biosaline agriculture: Mechanism, utilization, and value addition. Land Degrad Dev 29:1081–1095. https://doi.org/10.1002/ldr.2819
48. Ögren E, Baker NR (1985) Evaluation of a technique for the measurement of chlorophyll fluorescence from leaves exposed to continuous white light. Plant Cell Environ 8:539–547. https://doi.org/10.1111/j.1365-3040.1985.tb01691.x
49. Paez-Garcia A, Motes CM, Scheible W, Chen R, Blancaflor EB, Monteros MJ (2015) Root traits and phenotyping strategies for plant improvement. Plants 4:334–355. https://doi.org/10.3390/plants4020334
50. Pandey M, Chikara SK (2015) Effect of salinity and drought stress on growth parameters, glycoside content and expression level of vital genes in steviol glycosides biosynthesis pathway of *Stevia rebaudiana* (Bertoni). Int J Genet 7:153–160. https://doi.org/
51. Pereira MP, Rodrigues LCA, Corrêa FF, Castro CM, Ribeiro VE, Pereira FJ (2016) Cadmium tolerance in *Schinus molle* trees is modulated by enhanced leaf anatomy and photosynthesis. Trees 30:807–814. https://doi.org/10.1007/s00468-015-1322-0
52. Rahman A, Hossain MS, Mahmud JA, Nahar K, Hasanuzzaman M, Fujita M (2016) Manganese induced salt stress tolerance in rice seedlings: regulation of ion homeostasis, antioxidant defense and glyoxalase systems. Physiol Mol Biol Plants 22:291–306. https://doi.org/10.1007/s12298-016-0371-1
53. Rahman M, Rahman K, Sathi KS, Alam MM, Nahar K, Fujita M, Hasanuzzaman M (2021) Supplemental Selenium and Boron Mitigate Salt-Induced Oxidative Damages in *Glycine max* L. Plants 10:2224. https://doi.org/10.3390/plants10102224
54. Rewald B, Shelef O, Ephrath JE, Rachmilevitch S (2013) Adaptive plasticity of salt-stressed root systems. In: Ahmad P, Azooz MM, Prasad MNV (eds) Ecophysiology and responses of plants under salt stress. Springer, New York, pp 169–202. https://doi.org/10.1007/978-1-4614-4747-4_6
55. Rezende RALS, Rodrigues FA, Soares JDR, Silveira HRO, Pasqual M, Dias GMG (2018) Salt stress and exogenous silicon influence physiological and anatomical features of *in vitro*-grown cape gooseberry. Cienc Rural 48. https://doi.org/10.1590/0103-8478cr20170176

56. Ribera-Fonseca A, Rumpel C, Mora ML, Nikolic M, Cartes P (2018) Sodium silicate and calcium silicate differentially affect silicone and aluminium uptake, antioxidant performance and phenolics metabolism of ryegrass in an acid Andisol. Crop Pasture Sci 69:205–215. https://doi.org/10.1071/CP17202
57. Ribeiro VE, Pereira MP, De Castro EM, Corrêa FF, Cardoso MG, Pereira FJ (2019) Enhanced essential oil and leaf anatomy of *Schinus molle* plants under lead contamination. Ind Crop Prod 132:92–98. https://doi.org/ 10.1016/j.indcrop.2019.02.014
58. Rios JJ, Martínez-Ballesta MC, Ruiz JM, Blasco B, Carvajal M (2017) Silicon- mediated improvement in plant salinity tolerance: The role of aquaporins. Front Plant Sci 8:948. https://doi.org/ 10.3389/fpls.2017.00948
59. Rodrigues FA, Rezende RALS, Soares JDR, Rodrigues VA, Pasqual M, Silva SO (2017) Application of silicon sources in yam (*Dioscorea* spp.) micropropagation. Aust J Crop Sci 11:1469–1473. https://doi.org/10.21475/ajcs.17.11.11.pne685
60. Rouphael Y, Micco V, Arena C, Raimondi G, Colla G, Pascale S (2017) Effect of *Ecklonia maxima* seaweed extract on yield, mineral composition, gas exchange, and leaf anatomy of zucchini squash grown under saline conditions. J App Phycol 29:459–470. https://doi.org/10.1007/s10811-016-0937-x
61. Sahebi M, Hanafi MM, Azizi P (2016) Application of silicon in plant tissue culture. In Vitro Cell Dev Biol-Plant 52:226–232. https://doi.org/ 10.1007/s11627-016-9757-6
62. Santos ER, Martins JPR, Rodrigues LCA, Gontijo ABPL, Falqueto AR (2020) Morphophysiological responses of *Billbergia zebrina* Lindl. (Bromeliaceae) in function of types and concentrations of carbohydrates during conventional *in vitro* culture. Ornam Hort 26:18–34. https://doi.org/10.1590/2447-536X.v26i1.2092
63. Santos LR, Paula LS, Pereira YC, Silva BRS, Batista BL, Alsahli AA, Lobato AKS (2021) Brassinosteroids- Mediated Amelioration of Iron Deficiency in Soybean Plants: Beneficial Effects on the Nutritional Status, Photosynthetic Pigments and Chlorophyll Fluorescence. J Plant Growth Regul 40:1803–1823. https://doi.org/10.1007/s00344-020-10232-y
64. Sarruge JR, Haag HP (1974) Análise química de plantas. Departamento de Química- Escola Superior de Agricultura Luiz de Queiroz 56p, Piracicaba
65. Scholl J, Dengler L, Bader L, Forchhammer K (2020) Phosphoenolpyruvate Carboxylase from the cyanobacterium *Synechocystis* sp. PCC 6803 is under global metabolic control by P_{II} signaling. Mol Microbiol 114:1–16. https://doi.org/10.1111/mmi.14512
66. Schreiber U (1986) Detection of rapid induction kinetics with a new type of high-frequency modulated chlorophyll fluorometer. Photosynth Res 9:261–272. https://doi.org/10.1007/BF00029749
67. Shu S, Yuan R, Shen J, Chen J, Wang L, Wu J, Sun J, Wang Y, Shirong G (2019) The positive regulation of putrescine on light-harvesting complex ii and excitation energy dissipation in salt-

stressed cucumber seedlings. Environ Exp Bot 162:283–294. https://doi.org/10.1016/j.envexpbot.2019.02.027

68. Sivanesan I, Park SW (2014) The role of silicon in plant tissue culture. Front Plant Sci 5:1–4. https://doi.org/ 10.3389/fpls.2014.00571
69. Terletskaya N, Duisenbayeva U, Rysbekova A, Kurmanbayeva M, Blavachinskaya I (2019) Architectural traits in response to salinity of wheat primary roots. Acta Physiol Plant 41:157. https://doi.org/10.1007/s11738-019-2948-0
70. Tewari RK, Kumar P, Sharma PN (2019) An effective antioxidante defense provides protection against zinc deficiency-induced oxidative stress in Zn-efficient maize plants. J Plant Nutr Soil Sci 182:701–707. https://doi.org/10.1002/jpln.20180 0622
71. Wang Z, Li G, Sun H, Ma L, Guo Y, Zhao Z, Gao H, Mei L (2018) Effects of drought stress on photosynthesis and photosynthetic electron transport chain in young apple tree leaves. Biol Open 7:bio035279. https://doi.org/10.1242/bio.035279
72. Wellburn AR (1994) The spectral determination of chlorophylls *a* and *b*, as well as total carotenoids, using various solvents with spectrophotometers of different resolution. J Plant Physiol 144:307–313. https://doi.org/10.1016/S0176-1617(11)81192-2
73. Wu J, Guo J, Hu Y, Gong H (2015) Distinct physiological responses of tomato and cucumber plants in silicon-mediated alleviation of cadmium stress. Front Plant Sci 6:453. https://doi.org/ 10.3389/fpls.2015.00453
74. Yao J, Sun D, Cen H, Xu H, Weng H, Yuan F, He Y (2018) Phenotyping of Arabidopsis drought stress response using Kinetic Chlorophyll Fluorescence and Multicolor Fluorescence Imaging. Front Plant Sci 9:603. https://doi.org/10.3389/fpls.2018.00603
75. Zhao X, Bai X, Jiang C, Li Z (2019) Phosphoproteomic Analysis of Two Contrasting Maize Inbred Lines Provides Insights into the Mechanism of Salt-Stress Tolerance. Int J Mol Sci 20:1886. https://doi.org/10.3390/ijms20081886
76. Zeng Y, Li L, Yang R, Yi X, Zhang B (2015) Contribution and distribution of inorganic ions and organic compounds to the osmotic adjustment in *Halostachys caspica* response to salt stress. Sci Rep 5:13639. https://doi.org/ 10.1038/srep13639
77. Zushi K, Matsuzoe N (2017) Using of chlorophyll a fluorescence OJIP transients for sensing salt stress in the leaves and fruits of tomato. Sci Hortic 219:216–221. https://doi.org/10.1016/j.scienta.2017.03.016. https://doi.org/
78. Zhang Y, Liang Y, Zhao X, Jin X, Hou L, Shi Y, Ahammed GJ (2019) Silicon Compensates Phosphorus Deficit-Induced Growth Inhibition by Improving Photosynthetic Capacity, Antioxidant Potential, and Nutrient Homeostasis in Tomato. Agronomy 9:733. https://doi.org/10.3390/agronomia9110733
79. Zhu YX, Gong HJ, Yin JL (2019) Role of Silicon in Mediating Salt Tolerance in Plants: A Review. Plants 8:147. https://doi.org/10.3390/plants8060147

Figures

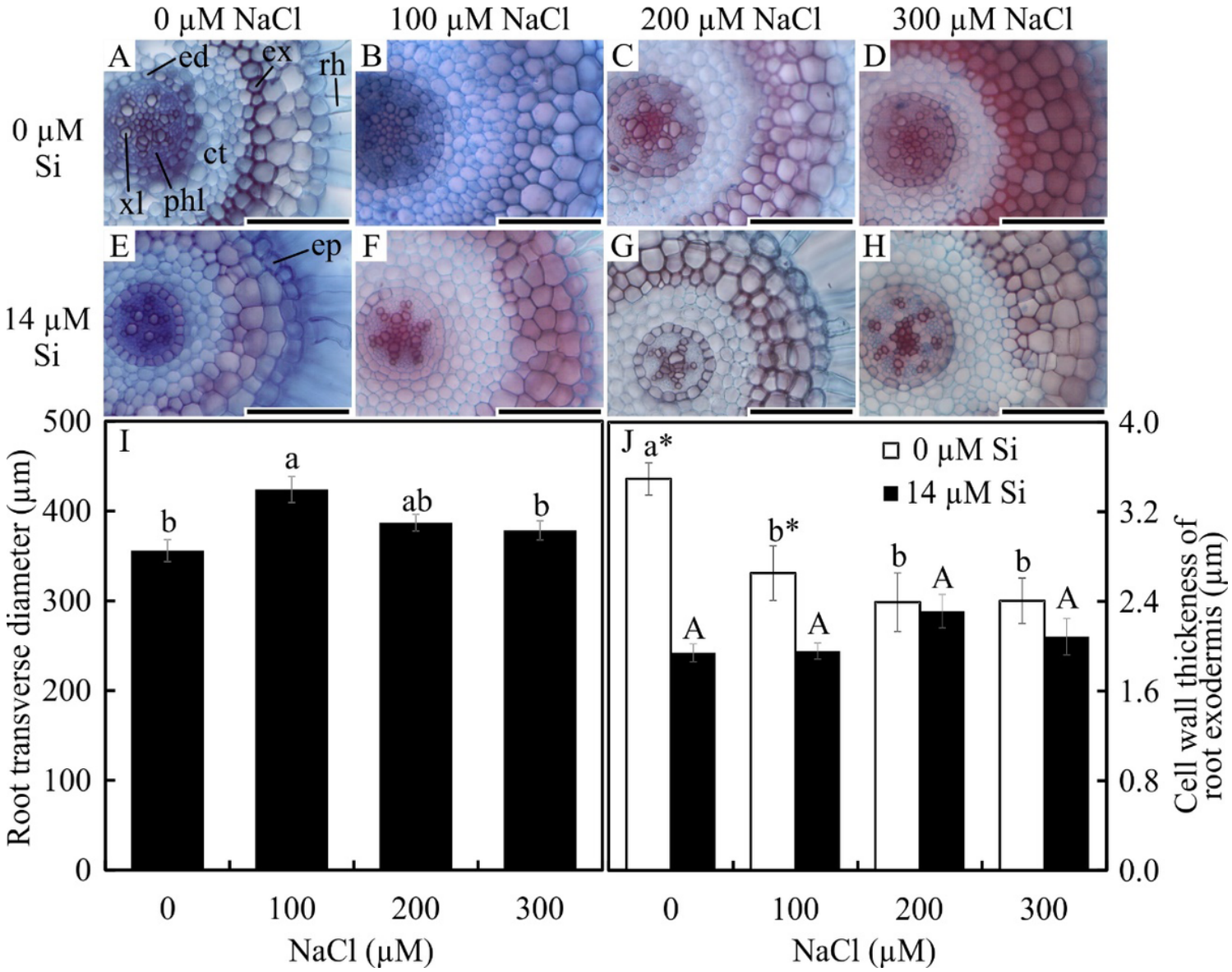

Figure 1

Cross-sections (A–H) and anatomical traits (I–J) of roots of *Aechmea blanchetiana* plants in the function of different concentrations of sodium chloride (NaCl) in the absence and presence of silicon (Si) during in vitro culture. Root transverse diameter (I) and cell wall thickness of root exodermis (J) of *Aechmea blanchetiana* in the function of the NaCl concentration (µM) and in the absence and presence of silicon (Si) during in vitro culture. (I) Means (± SE), *n* = 6, followed by the same letter do not differ according to the Tukey test at 5% significance. (J) Means (± SE), *n* = 6, followed by the same letter (lowercase for 0 µM Si and uppercase for 14 µM Si), at each NaCl concentration, do not differ according to the Tukey test at 5% significance. For each Si concentration analyzed (0 and 14 µM Si), the means followed by an asterisk are significantly different according to the Tukey test at 5% significance. ct – cortex, ed – endodermis, ep – epidermis, ex – exodermis, rh – root hair, xl – xylem, and, phl – phloem. Bars =100 µm.

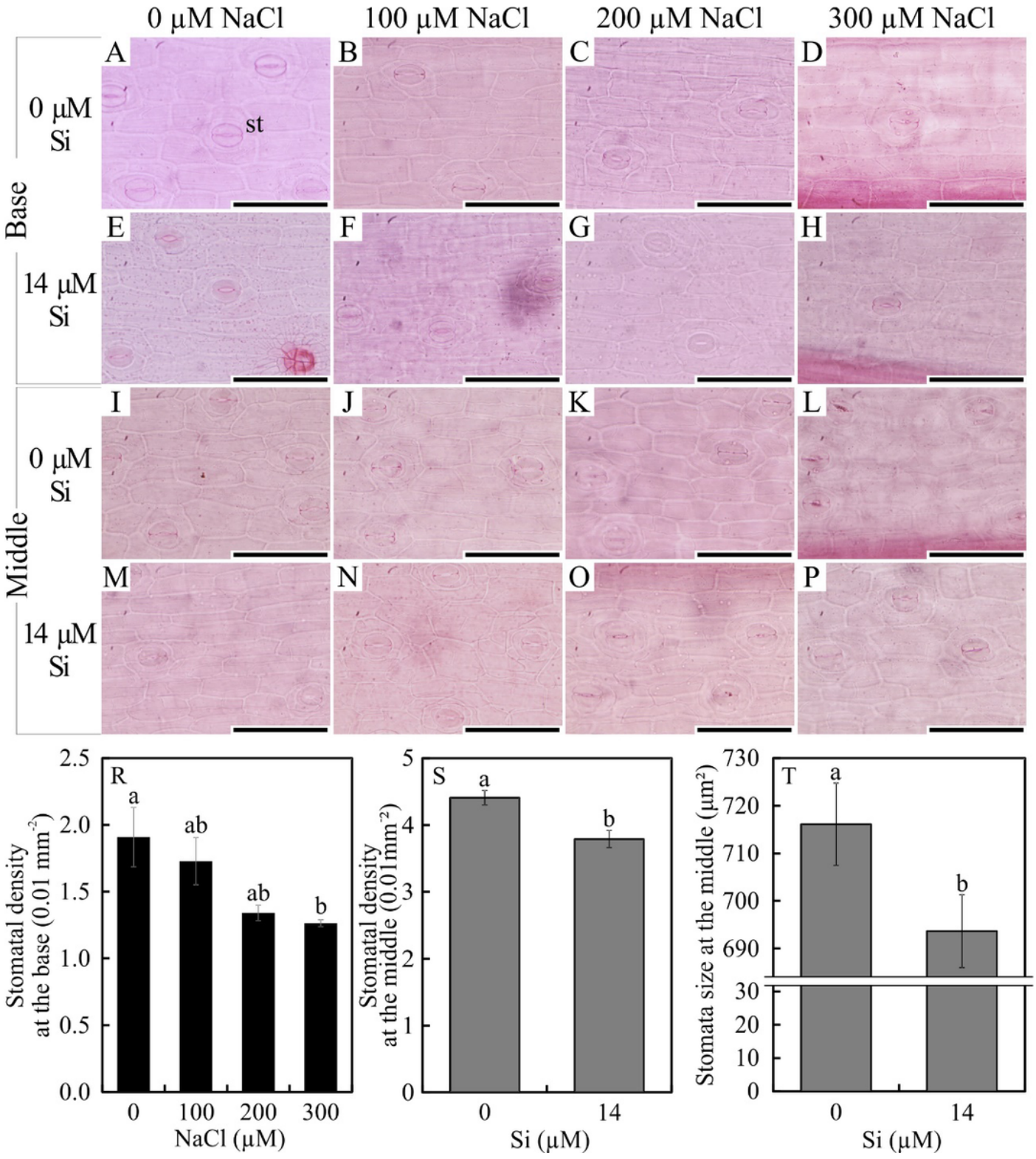

Figure 2

Paradermal sections (A – P) and stomatal traits of leaves of *Aechmea blanchetiana* plants in the function of different concentrations of sodium chloride (NaCl) in the absence and presence of silicon (Si) during in vitro culture. Means (± SE), *n* = 6, followed by the same letter do not differ according to the Tukey test at 5% significance. st – stomata. Bars = 100 µm.

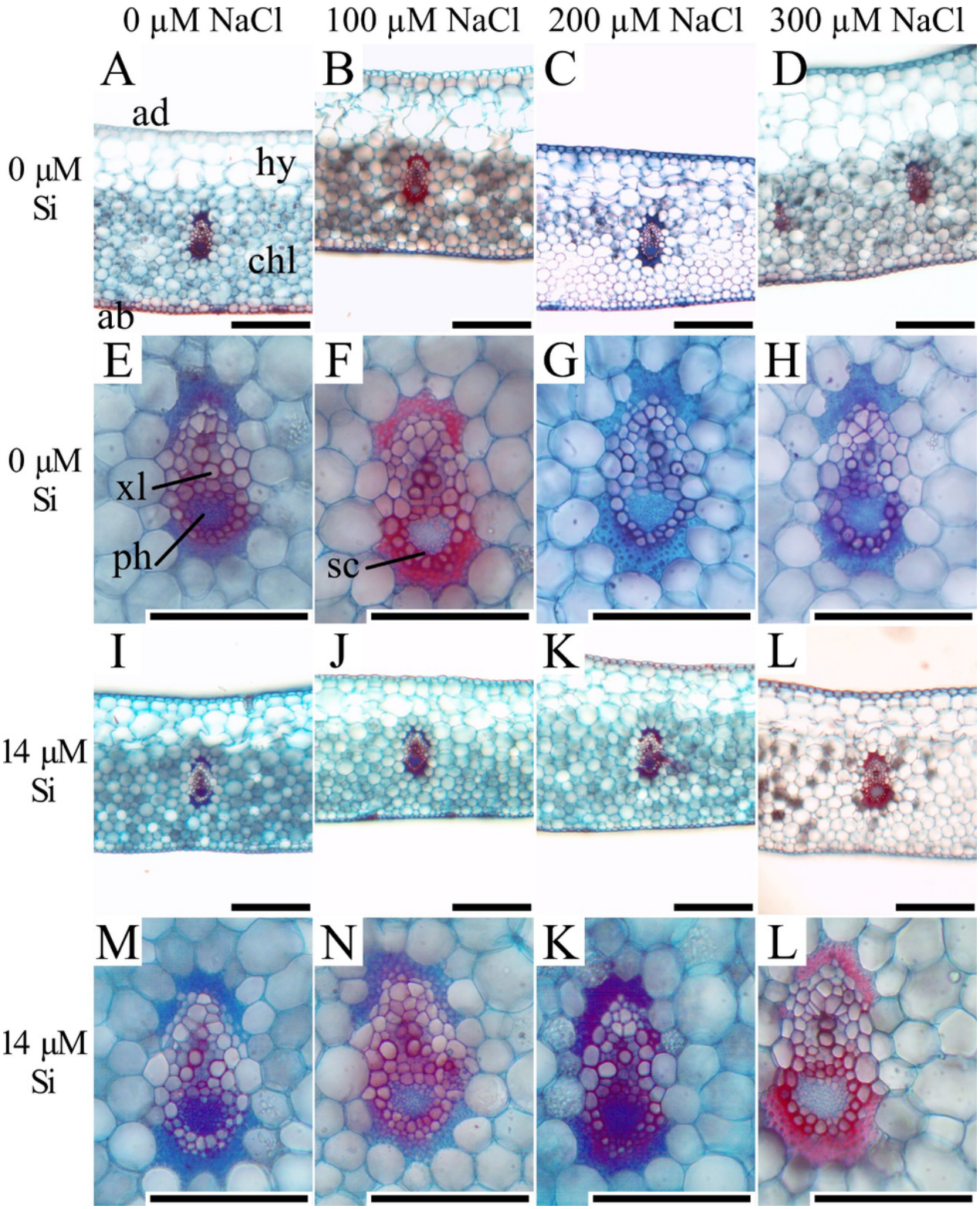

Figure 3

Cross-sections of leaves of *Aechmea blanchetiana* plants in the function of different concentrations of sodium chloride (NaCl) in the absence and presence of silicon (Si) during in vitro culture. ad – adaxial epidermis, ab – abaxial epidermis, chl – chlorenchyma, hy – hydrenchyma, ph – phloem, sc – sclerenchyma, xl – xylem. Bars = 100 µm.

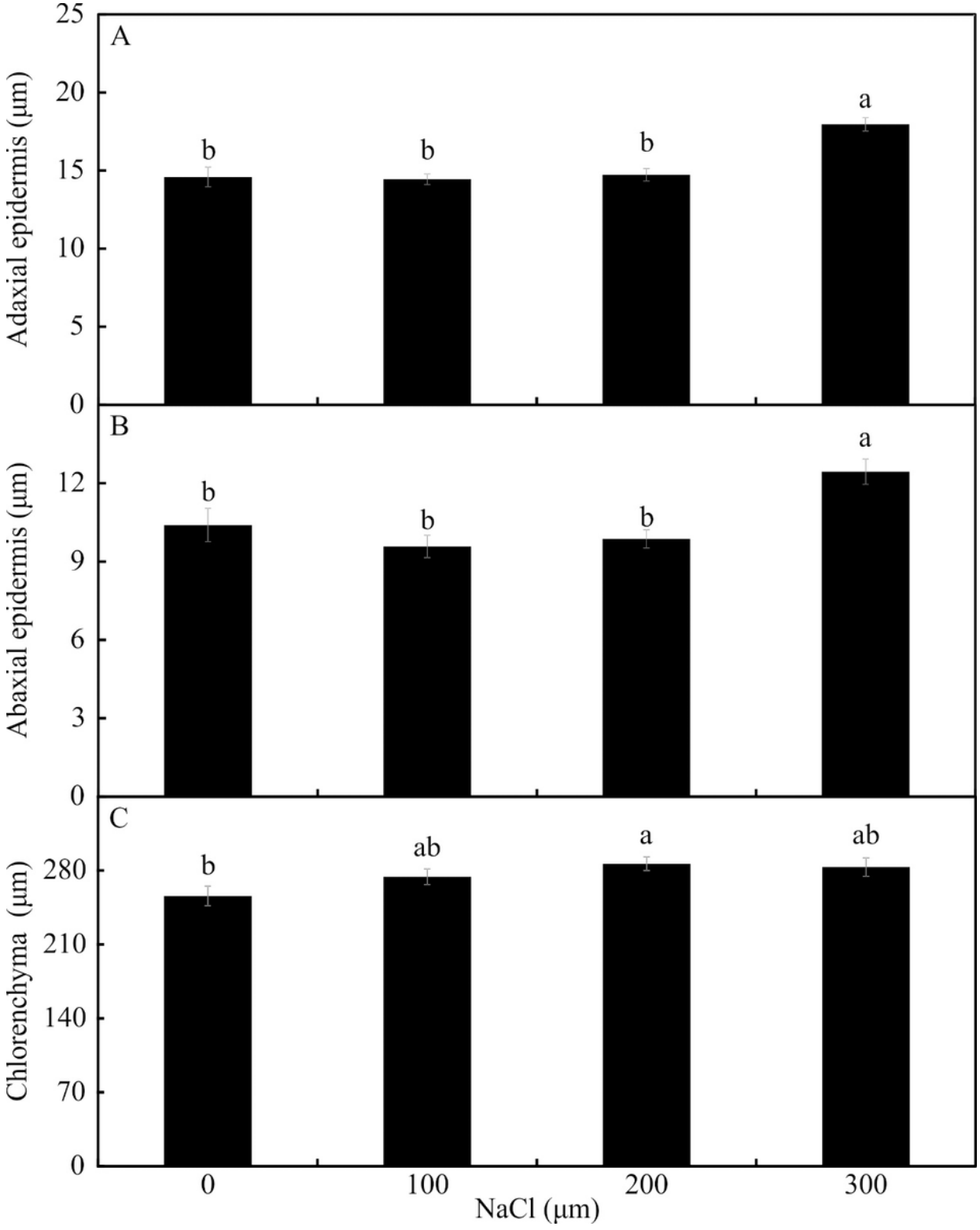

Figure 4

Thickness of the adaxial and abaxial faces of the epidermis (µM) (A – B) and the chlorenchyma (C) of leaves of *Aechmea blanchetiana* in the function of the concentrations of NaCl (0, 100, 200, 300 µM). Means (± SE), *n* = 6, followed by the same letter do not differ according to the Tukey test at 5% significance.

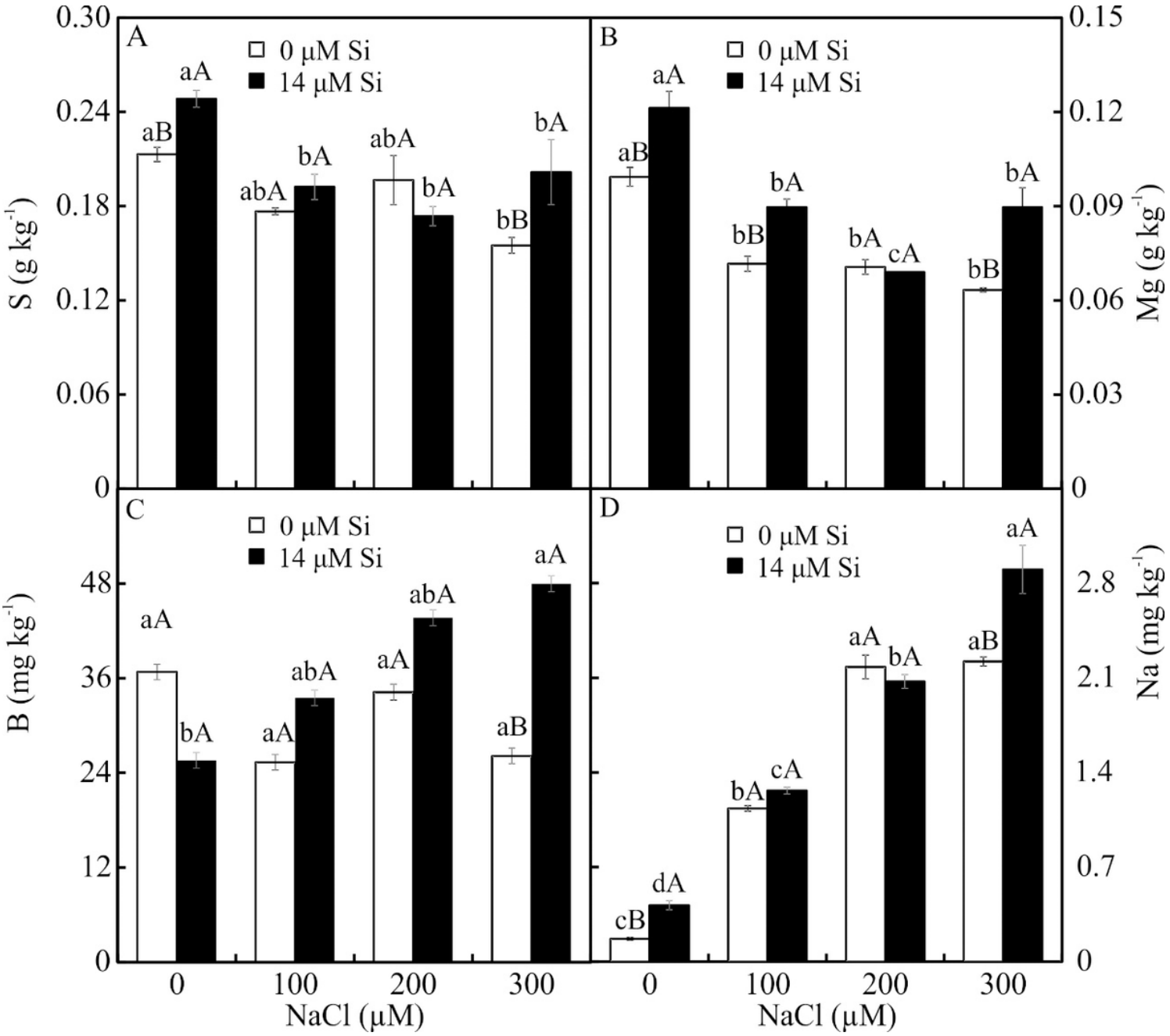

Figure 5

Contents of macronutrients and micronutrients in *Aechmea blanchetiana* plants in the function of NaCl concentrations (0, 100, 200, 300 µM) combined with 0 or 14 µM Si. For each nutrient, the means (± SE), *n* = 3, followed by the same lowercase letter (in the function of the NaCl concentration) and uppercase letter (in the function of the Si concentration), did not differ according to the Tukey test at 5% significance. S = sulfur, Mg = magnesium, B = boron, Na = sodium.

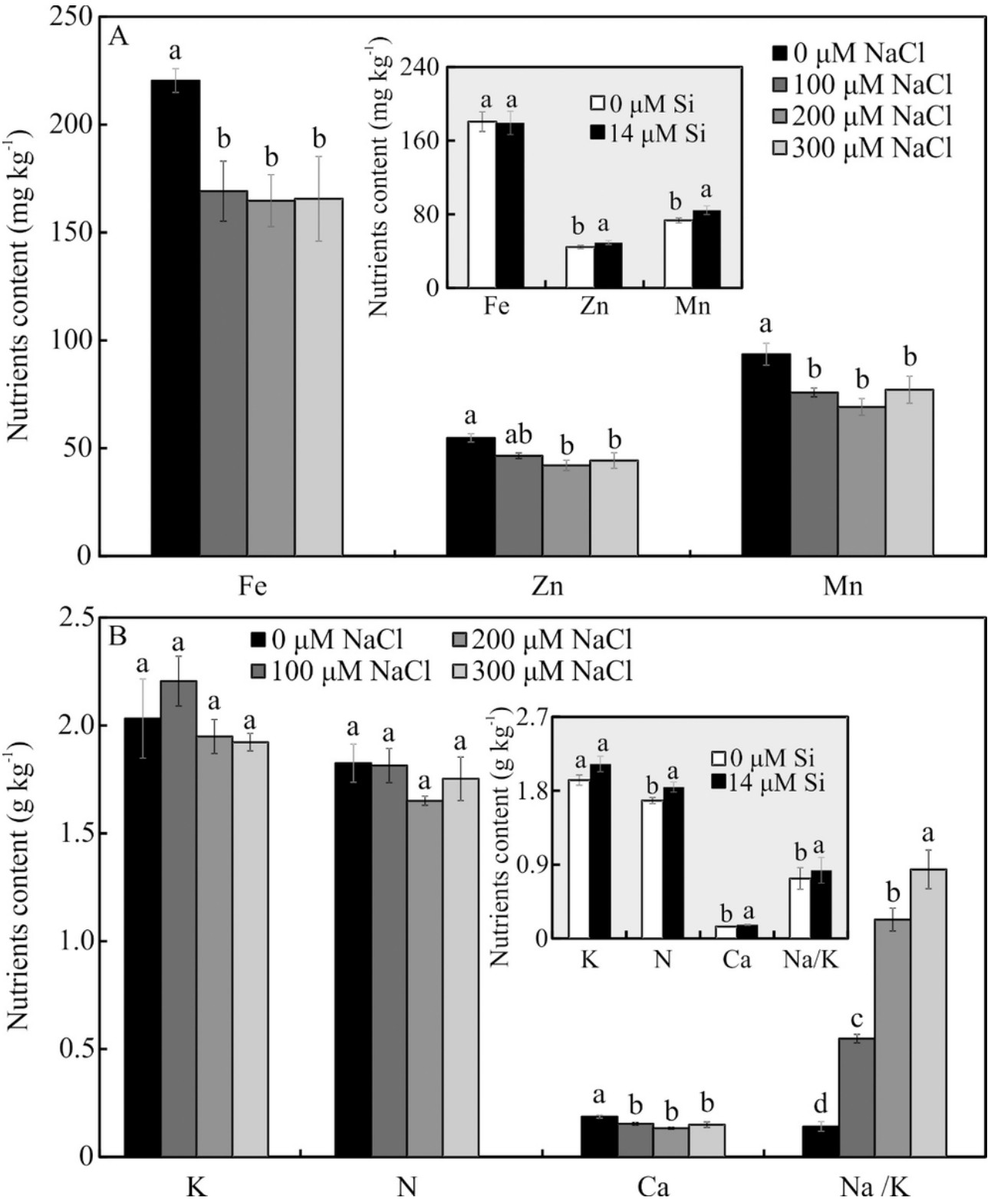

Figure 6

Contents of nutrients in *Aechmea blanchetiana* plants in the function of the concentrations of NaCl (0, 100, 200, 300 μM) or concentration of Si (0 or 14 μM Si). For each content of nutrients, the means (± SE), *n* = 3, followed by the same letter do not differ according to the Tukey test at 5% significance. Fe = iron, Zn = zinc, Mn = manganese, Ca = calcium, N = nitrogen, K = potassium, Na = sodium.

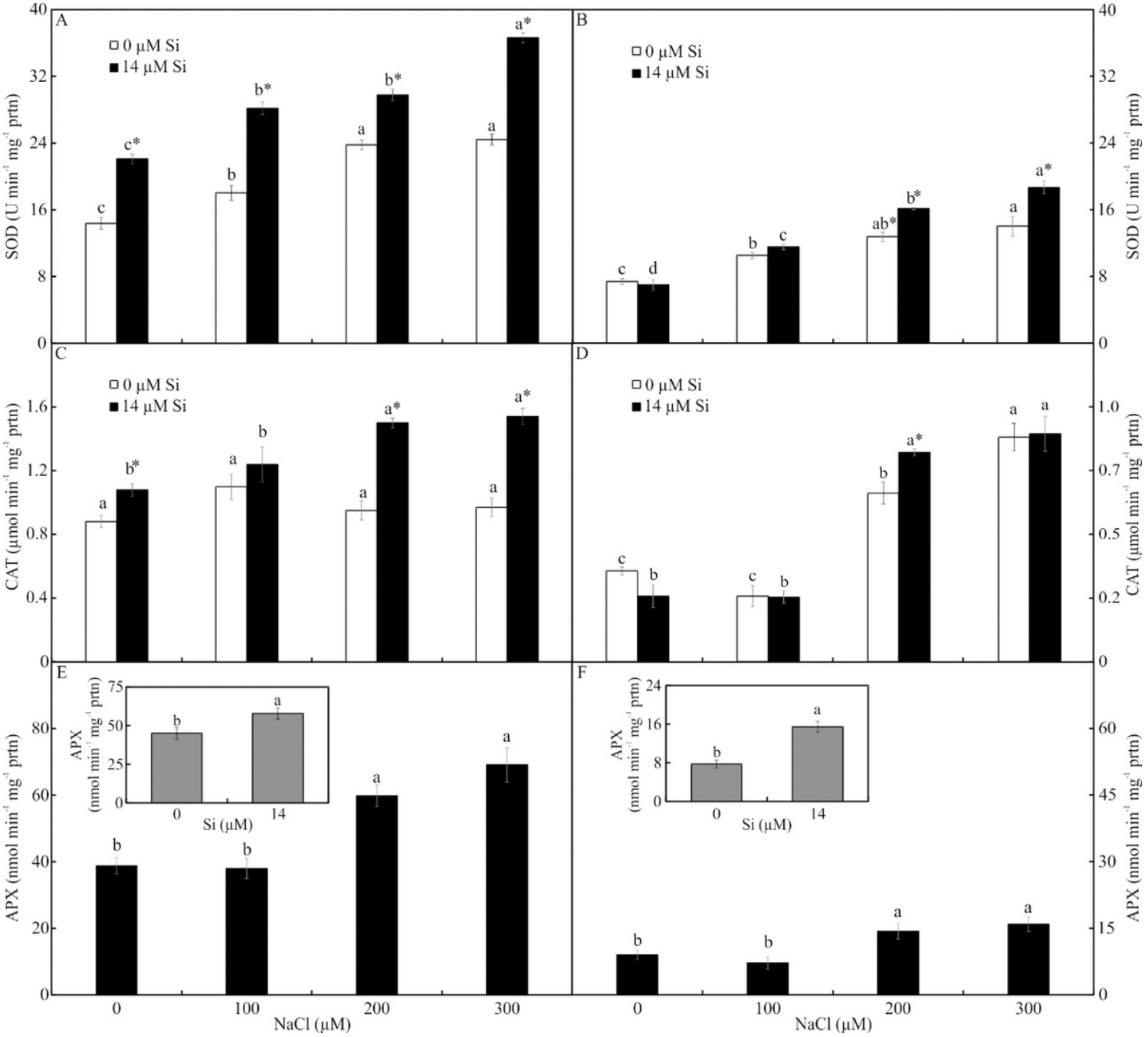

Figure 7

Activity of superoxide dismutase (SOD), catalase (CAT), and ascorbate peroxidase (APX) respectively in the leaves (A-C-E) and roots (B-D-F) of *Aechmea blanchetiana* plants cultivated in vitro in the function of the concentrations of NaCl (0, 100, 200, 300 µM) and concentration of Si (0 or 14 µM Si). Means (± SE), $n = 5$, followed by the same letter at each NaCl concentration, do not differ between Si content according to the Tukey test at 5% significance. For each Si concentration analyzed (0 and 14 µM Si), the means followed by an asterisk are significantly different according to the Tukey test at 5%.

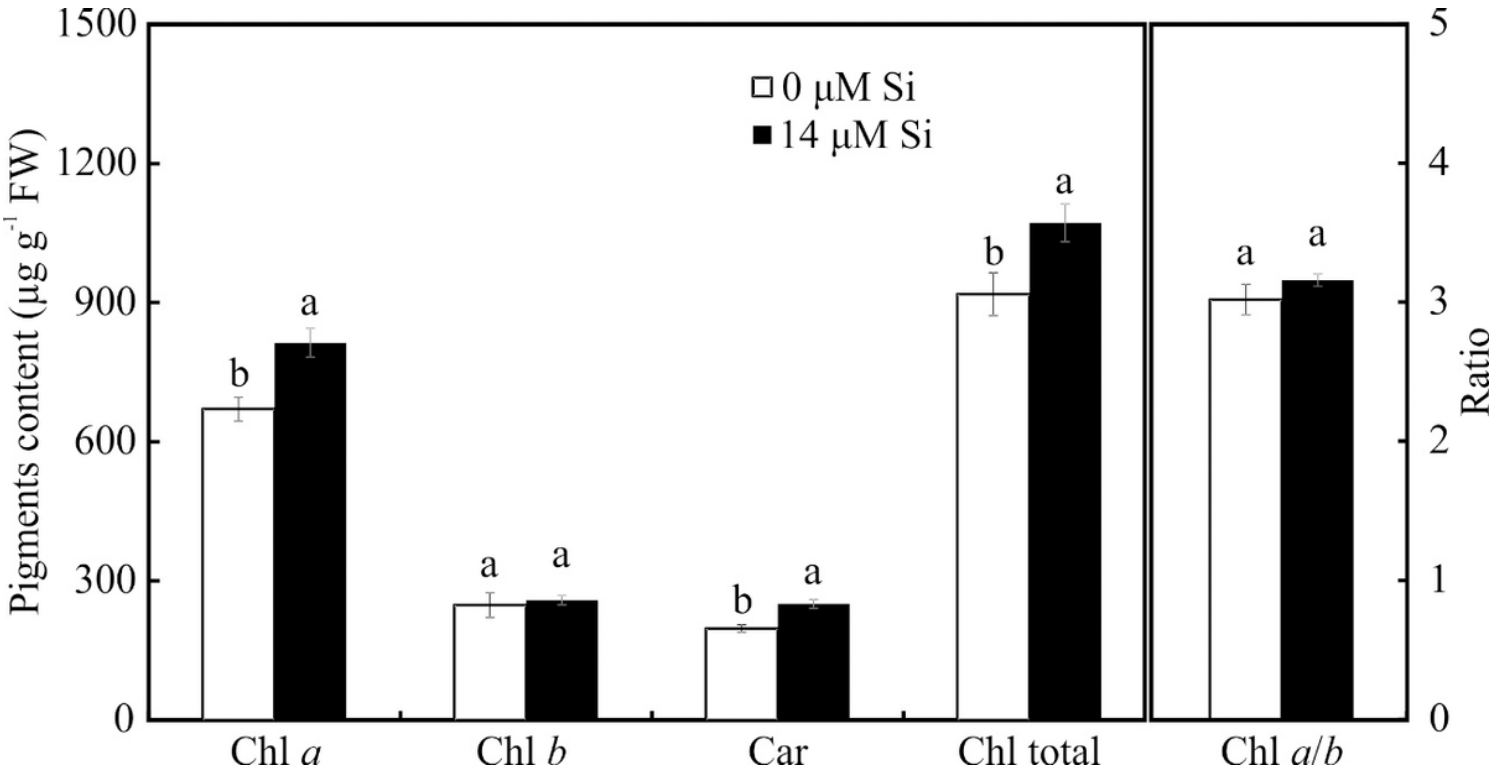

Figure 8

Contents of the photosynthetic pigments in *Aechmea blanchetiana* plants in the function of the presence or absence of Si (0 or 14 µM Si). Means (± SE), *n* = 8, followed by the same letter in each photosynthetic pigment, do not differ according to the Tukey test at 5% significance.

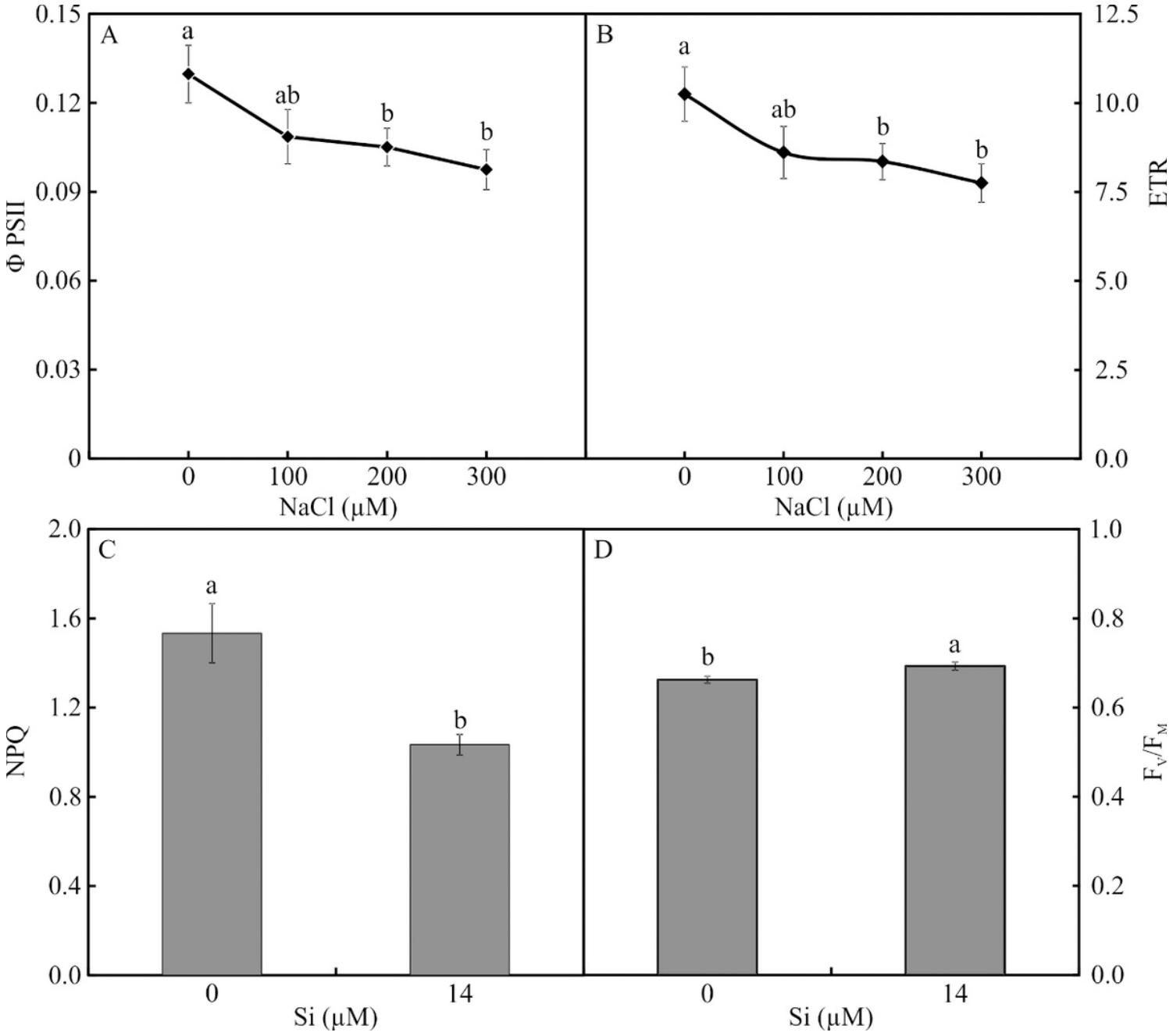

Figure 9

Effective photochemical quantum yield of PSII (ΦPSII) (A) and electron transport rate (ETR) (B) in the function of the concentrations of NaCl (0, 100, 200, 300 μM). Non-photochemical dissipation of fluorescence (non-photochemical quenching) (NPQ) (C) and maximum quantum yield of PSII (F_V/F_M) (D) in *Aechmea blanchetiana* plants in function of the presence or absence of Si (0 or 14 μM Si). Means (± SE), *n* = 12, followed by the same letter for each parameter, do not differ according to the Tukey test at 5% significance.

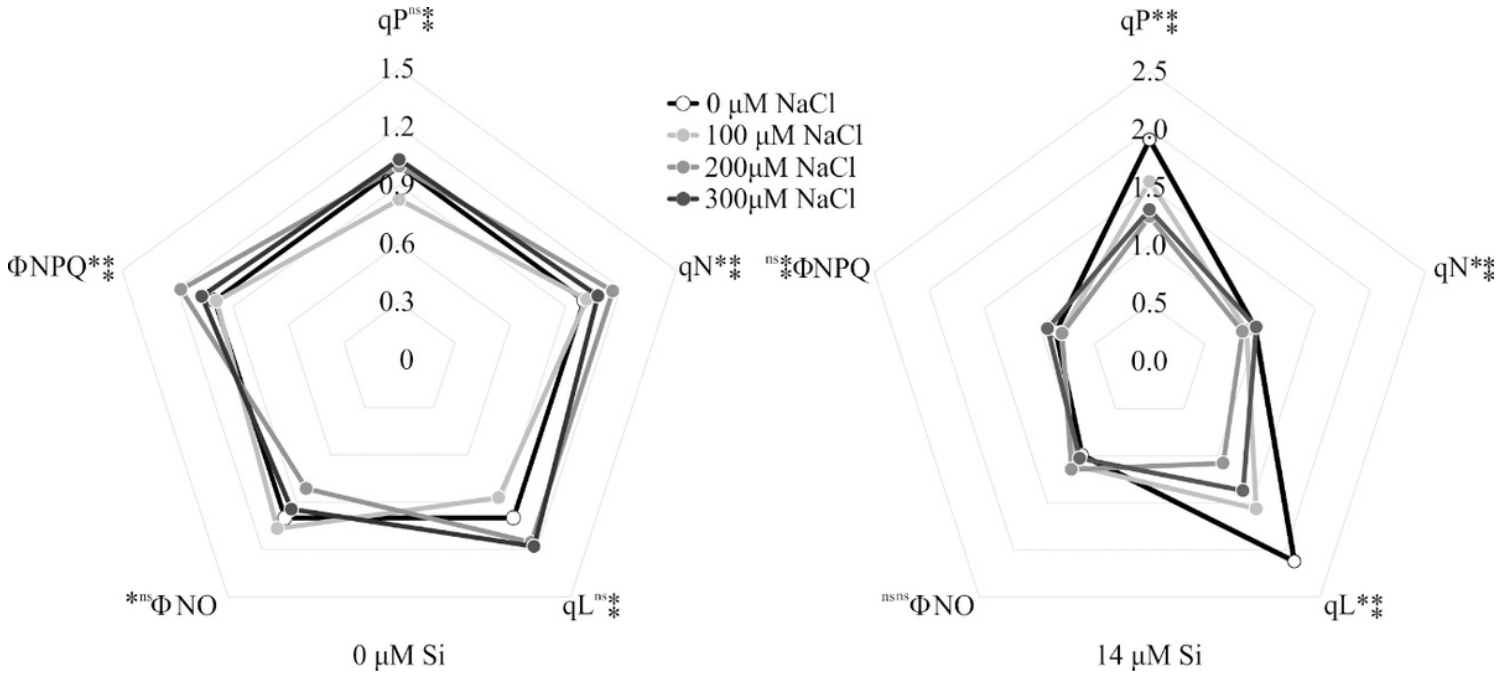

Figure 10

Modulated fluorescence parameters of *Aechmea blanchetiana* plants in the function of the concentrations of NaCl (0, 100, 200, 300 µM) combined with 0 µM Si (A) or 14 µM Si (B). For each parameter, means (n = 12) followed by an asterisk (*) denote significant differences between the concentrations of NaCl at each level of Si, while two asterisks ( ) denote significant differences between the presence and absence of Si according to the Tukey test at 5% probability. ns = no significant.

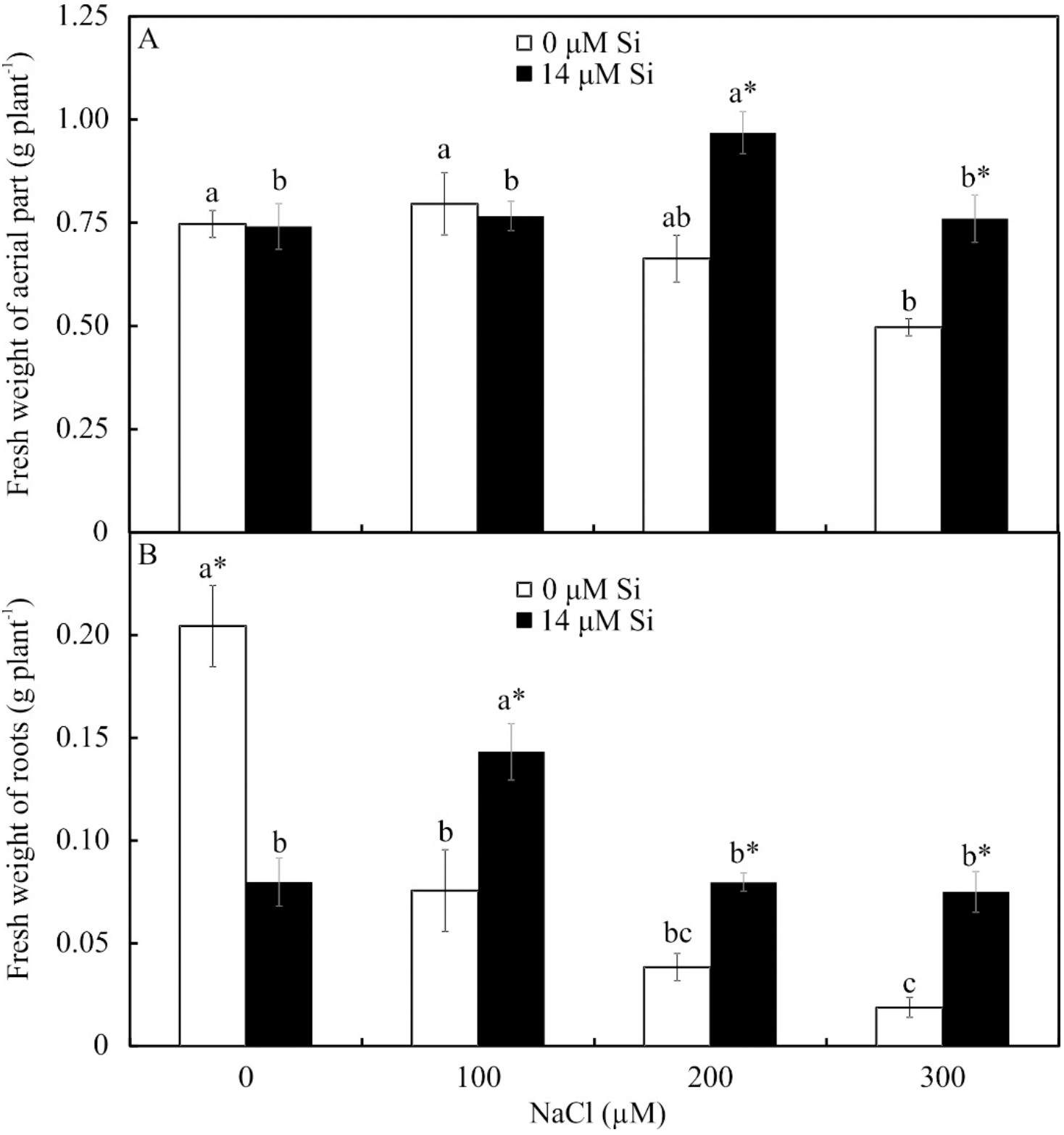

Figure 11

Shoot (A) and root (B) fresh weights of *Aechmea blanchetiana* plants in the function of the concentrations of NaCl combined with 0 or 14 µM Si. Means (± SE), *n* = 5, followed by the same letters (uppercase for plants grown with 0 µM Si and lowercase for plants supplemented with 14 µM Si) do not differ according to the Tukey test at 5% significance. For each Si concentration analyzed (µM), the means followed by an asterisk are significantly different according to the Tukey test at 5%.